

# PROTOTYPE OF AN AR-BASED SYSTEM FOR ENHANCED VISUALIZATION FUNCTIONALITY IN NAVIGATED NEUROSURGERY

Dr. Zein Salah, Prof. Dr. Bernhard Preim, Prof. Dr. Georg Rose

## Abstract

Neurosurgery obviously necessitates a high degree of precision. Therefore, surgical microscopes, in addition to medical navigation, are often used to support the safety and accuracy of such interventions. In this paper, we present a prototype for an AR system that provides enhanced visualization functionalities in an image-guided surgery by superimposing information, extracted from pre- and intra-operatively scanned patient data, with the optical microscope image. The advantage is a better localization of targeted lesions and the protection of hidden risk structures. To provide a more enhanced visualization, interactively selected tomographical slices can be computed on the fly and blended in the real scene. Overall, we already received promising positive feedback from our medical partners regarding the applicability of the system.

**Keywords:** Augmented Reality, Medical Data Visualization, Medical Navigation, Image-Guided Surgery

## 1. Introduction

Image-guided procedures receive a continuously increasing attention. In essence, image guidance helps physicians to establish a correspondence between locations in a patient dataset and the patient's physical body [Peters and Cleary, 2008]. This is of great importance for surgeries that necessitate a high degree of precision, like neurosurgery. For example, in a brain surgery, it is highly important to avoid injury of critical risk structures. Therefore, surgical microscopes, in addition to medical navigation, are usually used to support the safety and accuracy of such interventions [Brinker et al., 1998, Zheng et al. 2001].

By incorporating augmented reality (AR), it becomes possible to view patient data directly in the 3D context of the patient himself. This may provide an in-place insight into the patient body, which, for example, would help defining the entry point and the trajectory of a biopsy needle [Wacker et al., 2006]. In [Shahidi et al., 2002], a system for image-enhanced endoscopy was introduced. Particularly, the authors presented images from real paranasal endoscopy, paired with synthesized virtual renderings generated from the same view. A similar

approach was presented in [Lapper et al., 2008] with evaluation of the calibration, registration and tracking. A system for combining optical and virtual endoscopy was also introduced in [Fischer et al., 2007]. Birkfellner et al. [Birkfellner et al., 2002] presented a basic design of a head-mounted operating binocular that is equipped with projection optics to allow for data augmentation. In [Edwards et al., 2000], a see-through augmented view in a tracked microscope is achieved by incorporating a beam-splitter.

In this paper, we first present an efficient algorithm for computing cross sectional slices from volumetric datasets. We then integrate this algorithm into an augmented reality based visualization module, which allows for interactively browsing and inspecting 3D datasets. In essence, the dataset as well as other tools (e.g. pointers) are optically tracked with a camera and cross sections are computed and visualized in correspondence with the tracked pointers. If the dataset is registered with the corresponding real patient, it becomes possible to display the tomographical slices in correspondence with the patient body.

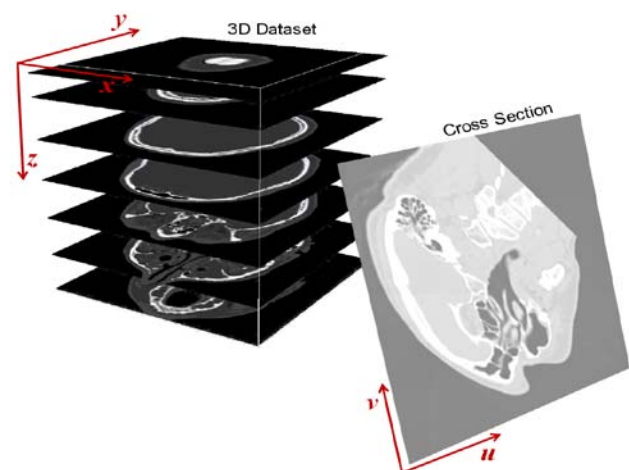


Figure 1: Arbitrarily-oriented slices are computed from volumetric datasets.

In a next step, the AR-assisted visualization module is extended to a prototype of a PC-based prototype for augmenting information, extracted from pre- and intra-operatively scanned patient data, with the optical microscope image. The advantage is a better localization of targeted lesions (e.g. tumor) and the protection of

hidden risk structures like blood vessels and neural connections. To provide a more enhanced visualization, interactively selected tomographical slices can be computed on the fly and blended in the real scene with correct position and orientation.

The remainder of this paper is organized as follows: Section 2 provides a detailed description of the material and methods. The cross section computation algorithm is presented in Section 3.1. In section 3.2, the AR-assisted system for slice visualization is presented, whereas in Section 3.3, this system is extended to a prototype for enhanced visualization in neurosurgery. Section 4 gives some notes on implementation issues and presents representative results. Finally, the paper is concluded in Section 5.

## 2. Material and Methods

### 2.1. Computation and Rendering of Tomographical Slices

The first component of the system is an algorithm (CSGenerator) for computing cross sectional tomographical slices from 3D CT/MRI datasets. The inputs of the CSGenerator are a 3D dataset and the parameters of the desired cross section (center, orientation, dimensions, and sampling rate), and the output is the computed 2D cross section. The first algorithm implementation computes, given the a.m. input parameters, a 4x4 transformation matrix  $T_{cs}$ , which converts from the coordinate system of the cross section to that of the volume.  $T_{cs}$  is applied to every pixel position  $Index2D$  in the cross section coordinates, and the intensity at the output continuous 3D position  $ContIndex3D = T_{cs} * Index2D$  is computed using tri-linear interpolation.

For better performance, we alternatively use  $ContIndex3D$  as an iteration counter and compute its value only at the lower-left pixel in the cross section plane. We also predefine two increment 3D vectors:  $Inc_x$ , which moves the counter a one-pixel step to the right, and  $Inc_y$ , which moves it to the left-most pixel in the next row. Notice that floating point multiplications are avoided using this approach, since looping through the pixels of the 2D slice plane is achieved using vector addition, which obviously reduces the computation time.

### 2.2. AR-Assisted Slicer

The AR-assisted slicer (AR-Slicer) allows for the inspection of a tracked 3D dataset by virtually browsing it using a tracked pointer. For our prototype, we use an off-the-shelf web camera, which corresponds to a microscope or endoscope in an AR-assisted navigated surgery. A main challenge in the AR-system is the precise computation of the viewpoint of the camera, in order to exactly align virtual objects with real world images. We utilize the ARToolkit for this purpose.

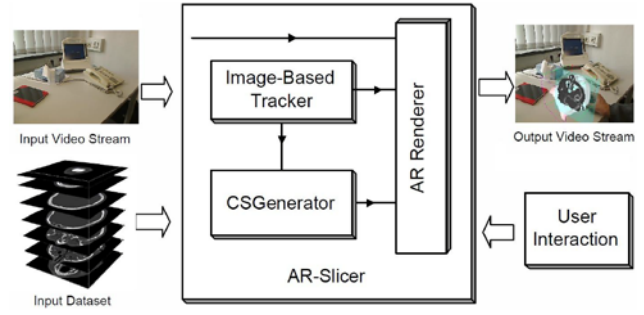


Figure 2: AR-Slicer: Using a tracked marker, the user interactively browses a volumetric dataset, which is augmented in the video stream, and the computed tomographical slices are blended in correct position and orientation within the scene.

The AR-Slicer is illustrated in Figure 2. The input video stream is captured with the camera and continuously rendered as a background. At each video frame, the image-based tracker searches for and detects predefined markers in the image and computes, for each visible marker, the 3D position and orientation (pose) and provides this information in the form of a 4x4 homogenous transformation matrix.

In our scenario, two trackable markers are used: a reference and a pointer marker. The pose matrix of the reference marker  $T_{ref}$  is used to align the dataset (e.g. the face and bounding box in Figure 3). The pose matrix of the pointer marker  $T_{pointer}$ , is used to align the computed tomographical slice. The input parameters of the CSGenerator algorithm (Section 3.1) are extracted from a relative transform  $T_{relative}$ , which is computed as

$$T_{relative} = T_{pointer} * T_{ref}^{-1}.$$

i.e.  $T_{relative}$  represents the pose data of the cross section in the coordinate system of the 3D dataset. Finally, the generated cross sectional image is used as texture for a rectangle, which is in turn rendered in the real scene using the transformation  $T_{pointer}$ .

The transformation matrices above are all computed in the world coordinate system (camera coordinate system), which is represented in millimeter. In order for the virtual objects (dataset bounding box, skin and cross sections) to be rendered with the correct scaling within the scene, the resolution of the original dataset, i.e., dimension and pixel size, are taken into consideration during cross section generation as well as rendering.

### 2.3. Prototype for AR-Enhanced Visualization in Neurosurgery

In this section, we extend the AR-Slicer (Section 3.2) to form the core of a prototype for improving visualization functionality in a simulated surgery scenario, in which we rely on two operational datasets and surgical microscope images. In a preprocessing step, we segment a malign brain tumor from a preoperative MRI dataset, which was

scanned directly prior to the real operation, where the setup of the operation room allows for registering multiple pre- and intraoperative scans. The intraoperative MRI was scanned directly before tumor resection has been started. From this MRI, we segment and reconstruct the outer skin with the Marching cubes algorithm [Lorensen and Cline, 1987]. The operation field in the reconstructed model is then textured with corresponding real microscope images to finally build a virtual patient model. Obviously, the patient model is inherently registered with the scanned dataset.

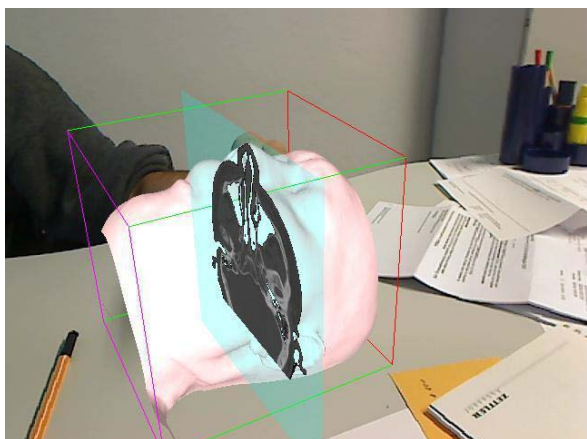


Figure 3: AR-Slicer: The face and bounding box of a CT dataset are blended into the video stream. A marker is used as a pointer to interactively select slices within the dataset.

We use a marker to track the virtual patient model and, at each frame, the patient model is blended into the real image and the depth buffer is cleared, which results in having the patient rendering as part of the real image. At this step, the new rendering simulates a frame captured during a real intervention. Additional object models segmented from MRI datasets, as well as interactively selected cross sections can be superimposed on the real image with exact position and orientation, as will be demonstrated in the next section.

### 3. Implementation and Results

The system and algorithms presented in this paper have been implemented with C++ (Microsoft Visual Studio 2005). To test the cross section generation algorithm (Section 3.1), an interactive software module was implemented using FLTK<sup>1</sup> for the GUI. Segmentation operations (e.g. of the tumor in Section 3.3) were performed utilizing a semiautomatic approach, partially based on Kitware's Insight Segmentation and Registration Toolkit ITK<sup>2</sup>. Reconstruction of 3D models of the skin and tumor was performed using the implementation the Marching Cubes algorithm provided by the Visualization Toolkit VTK<sup>3</sup>. For our current implementation of the

prototype, we relied on marker-based tracking provided by the ARToolkit<sup>4</sup>. Rendering was performed using OpenGL<sup>5</sup>, where the GUI, shown in Figure 4, was implemented using the Qt<sup>6</sup> library.

For datasets with 512x512 pixels and an average of 100 slices, the computation and display of cross sections (Section 3.1) of 512x512 pixels run in about 7 frames per seconds (fps). Using the optimized implementation, the computation and rendering rate was accelerated to about 30 fps.

The ARToolkit allows for multiple-marker tracking in real time. For capturing the input video stream, we used a Logitech QuickCam 9000 Pro Webcam, and image resolution was defined as 640x480 pixels. The AR-Slicer allows for intuitively inspecting 3D datasets by rendering interactively selected cross sectional slices, where a marker is used as a pointer for this purpose. An example of such cross sections is demonstrated in Figure 3. From an implementation point of view, the AR-Slicer is incomparably simpler than the system presented in [Shukla et al., 2009]. Nevertheless, it is more intuitive and can practicably be used to align tomographical slices directly with the corresponding patient.

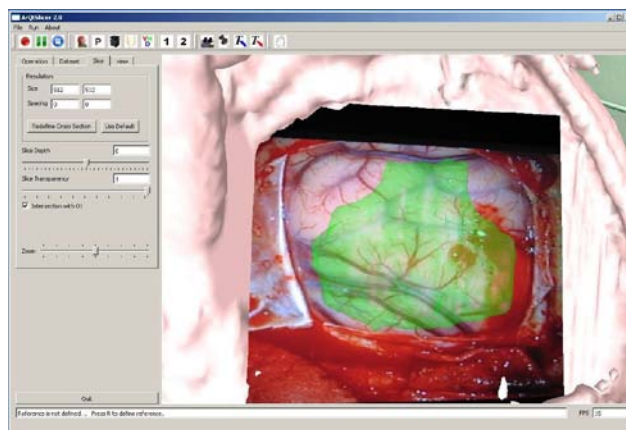


Figure 4: Snapshot of our AR-assisted prototype of the visualization system. A model of a previously segmented tumor (green) is superimposed on the operation field. The OP microscopy image was acquired in a tumor surgery at the INI<sup>7</sup> Hannover (Prof. M. Samii).

Figure 4 shows a snapshot of our prototype for enhanced visualization functionality in an operation scenario. The widget at the right side shows an augmented view of a malignant tumor (green). Obviously, this augmentation allows for a better delineation of the tumor boundaries and hence for a more protective resection. Additionally, it is highly important to protect risk structure like blood vessel or certain functional unit, which may be invisible. For this purpose, our prototype allows for augmenting slices of the patient anatomy, aligned directly with the operation region

<sup>1</sup> <http://www.fltk.org/>

<sup>2</sup> <http://www.itk.org/>

<sup>3</sup> <http://www.vtk.org/>

<sup>4</sup> <http://www.hitl.washington.edu/artoolkit/>

<sup>5</sup> <http://www.opengl.org/>

<sup>6</sup> <http://qt.nokia.com/>

<sup>7</sup> International Neuroscience Institute.

of interest. These slices are computed orthogonally to the viewing direction. In Figure 5, a transparent tomographical slice is computed at a depth of 11 mm below the focus plane, and superimposed on the operation field, where this depth can be controlled interactively.

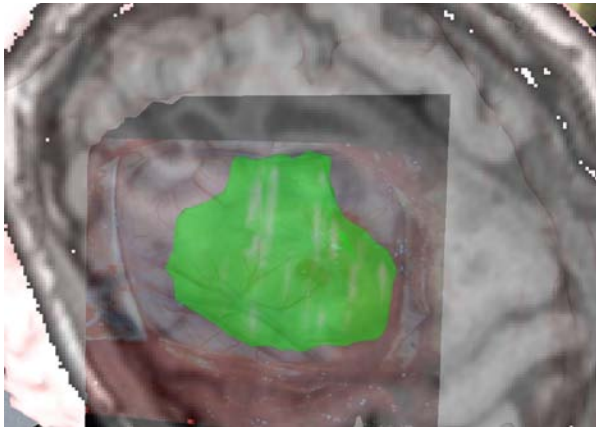


Figure 5: A tomographical slice is computed perpendicular to the viewing vector, at a depth of 11 mm relative to the focus plane, and superimposed on the operation field, together with an augmented view of the tumor.

#### 4. Conclusion

A system for an AR-assisted slice visualization, based on an efficient cross section computation algorithm, has been presented in this paper. The system has then been adapted for use in a simulated operation scenario by augmenting information extracted from scanned patient data with optical microscope images. This results in a better localization of targeted lesions and the preservation of high risk anatomical structures. We already received positive feedback from our medical partners regarding the good usability of the system. In a real surgery suite the surgical microscope will replace the camera and the camera tracking will be performed by an infrared tracking system. Although, the system initially was aimed for neurosurgery application the concept can be transferred to several other surgery procedures. Currently, we are exploring the application of this framework within abdominal endoscopic surgeries.

#### Acknowledgment

This work is funded by the German Ministry of Education and Science (BMBF) within the ViERforES project (no. 01IM08003C). We thank Prof. Rudolf Fahlbusch and Prof. Amir Samii for the fruitful clinical cooperation, for providing medical image data, insights in medical procedures, feedback for our prototype and further ideas.

#### References

[1] Birkfellner W, Figl M, Huber K, Watzinger F, Wanschitz F, Hummel J, Hanel R, Greimel W, Homolka P, Ewers R, Bergmann H, 2002, A Head-Mounted Operating Binocular for Augmented Reality Visualization in Medicine-Design

and Initial Evaluation. *IEEE Transactions on Medical Imaging*, 21(8):991–997.

[2] Brinker T, Arango G, Kaminsky J, Samii A, Thorns U, Vorkapic P, Samii M, 1998, An Experimental Approach to Image Guided Skull Base Surgery Employing a Microscope-Based Neuronavigation System. *Acta Neurochirurgica*, 140(9):883–889.

[3] Edwards P, King A, Maurer C, de Cunha D, Hawkes D, Hill D, Gaston R, Fenlon M, Chandra S, Strong A, Chandler C, Gleeson M, 2000, Design and Evaluation of a System for Microscope-Assisted Guided Interventions (MAGI). *IEEE Transactions on Medical Imaging*, 19(11):1082–1093.

[4] Fischer J, del R'io A, Neff M, Flossmann S, Duffner F, Hoffmann J, Straser W, Bartz D., 2007, The ARGUS System: Surgical Mixed Reality based on Image Guided Surgery, Extensions, and Applications. In: *Proc. of Computer-Aided Surgery around the Head (CAS-H)*.

[5] Lapeer R, Chen M, Gonzalez G, Linney A, Alusi G., 2008, Image-Enhanced Surgical Navigation for Endoscopic Sinus Surgery: Evaluating Calibration, Registration and Tracking. *The International Journal of Medical Robotics and Computer Assisted Surgery*, 4(1):32–452.

[6] Lorensen W., Cline H., 1987, Marching Cubes: A High Resolution 3D Surface Construction Algorithm. In *Proc. of ACM SIGGRAPH*, pages 163–169.

[7] Peters T, Cleary K., 2008, *Image-Guided Interventions, Technology and Applications*. Springer Science+Business Media.

[8] Shahidi R, Bax MR, Maurer C, Johnson J, Wilkinson E, Wang B, West J, Citardi M, Manwaring K, Khadem R., 2002, Implementation, Calibration and Accuracy Testing of an Image-Enhanced Endoscopy System. *IEEE Transactions on Medical Imaging*, 21(12):1524–1535.

[9] Shukla G, Wang B, Galeotti J, Klatzky R, Wu B, Unger B, Shelton D, Chapman B, Stetten G., 2009, A Movable Tomographic Display for 3D Medical Image. In: *Proc. of AMI-ARCS*.

[10] Wacker F, Vogt S, Khamene A, Jesberger J, Nour S, Elgort D, Sauer F, Duerk J, Lewin J., 2006, An Augmented Reality System for MR Image-guided Needle Biopsy: Initial Results in a Swine Model. *Radiology*, 238(2):497– 504.

[11] Zheng G, Caversaccio M, Bächler R, Langlotz F, Nolte L, Häusler R., 2001, Frameless Optical Computer-Aided Tracking of a Microscope for Otorhinology and Skull Base Surgery. *Archives of Otolaryngology - Head and Neck Surgery*, 127(10):1233–1238.